In Vivo Sodium MR Imaging of Rabbit Kidney using Dual-tuned RF Coil at 3T

C. Moon[1], A. Furlan[1], J-H. Kim[1], L. Jacobs[2,3], T. Zhao[4], and K. Bae[1]

[1]Radiology, University of Pittsburgh, Pittsburgh, PA, United States, [2]Orthopaedic Surgery, University of Pittsburgh Medical Center, Pittsburgh, PA, United States,

[3]Ferguson Laboratory for Orthopaedic and Spine Research, [4]MR Research Support, Siemens Healthcare, Pittsburgh, PA, United States

[Introduction] The kidney regulates the homeostasis of body fluids and electrolytes which builds up the corticomedullary gradient of extracellular sodium concentration. Sodium MR imaging may potentially be useful to evaluate renal function and diagnose renal diseases because it allows us to non-invasively measure sodium concentration changes in vivo within the kidney [1-3]. However, sodium MR imaging can be challenging because it is technically difficult and the intrinsic MR sensitivity to sodium nuclei is low. In this study, we determined the feasibility of high-resolution sodium MR imaging of rabbit kidneys (~2×2×4 cm^3) on a 3T human scanner using a high-sensitive dual-tuned (DT) RF coil and ultra-short echo time (UTE) spiral sequence.

[Methods and materials] All scans were performed using a 3T human scanner (Siemens Medical Solutions, Germany). Five New Zealand white rabbits were studied: <1 year old, female, and 5.2 + 0.4 kg. The rabbits were anesthetized for 120 to 150 min with ketamine 20 mg/kg, xylazine 4mg/kg, and acepromazine 1mg/kg. Proton/sodium MR imaging was performed using a multi-channel DT RF coil (designed for human knee imaging) at 3T clinical scanner. DT coil consisted of 4-ch proton and 8-ch sodium with 120-mm diameter and 150-mm height [4]. Rabbits fit snugly in the coil and were positioned supine to the center of coil. Foam pads were inserted to immobilize the body during the scan. Proton scout and T2-weighted TSE (or DESS) image (**Figs. 1A - C**) were acquired; TSE – TR/TE = 3500/109 ms, resolution = 0.6×0.6×3 mm^3; DESS – TR/TE = 14/5 ms, resolution = 0.6×0.6×3 mm^3. For the sodium MR imaging (**Figs. 1D - F**), the same shim values as the proton imaging were applied; 3D UTE spiral sequence [5], RF hard pulse of 500-μs duration, TR/TE = 100 – 150/0.27 ms, readout time T_{RO} = ~15 ms, resolution = 2 mm^3, and TA = 27 min. For the quantification of sodium concentration in the kidney, a homogeneous cylindrical phantom filled with 4% agar with 30-mM [^{23}Na] (120-mm diameter and 150-mm height) was used for B_1 field inhomogeneity correction (**Fig. 2A**). Sodium images of rabbits were co-registered on the phantom images on basis of eight 60-mM [^{23}Na] reference markers (5 cc syringe) that were placed on the wall of sodium coil frame. The signal reduction due to sodium T_1 and T_2 relaxation time (17.6 ms and 9.7 ms, respectively) was simulated based on 4% agar with 153-mM [$_{23}$Na] and used to compensate for the quantitative sodium imaging (**Fig. 2**). Sodium distribution in the kidney from cortex to medulla (**Fig. 3**) was measured as well as the total sodium concentration in the rabbit kidney (**Fig. 2C**).

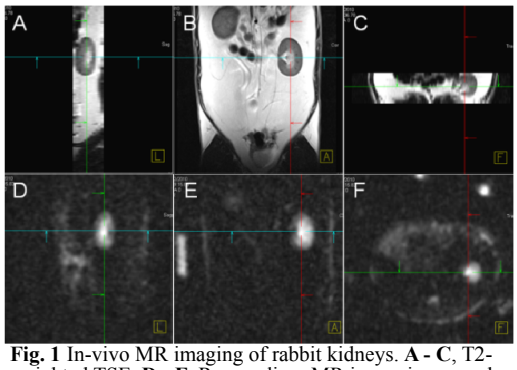

Fig. 1 In-vivo MR imaging of rabbit kidneys. **A - C**, T2-weighted TSE. **D - F**, Raw sodium MR image in coronal sagittal, and axial view; UTE spiral sequence, TR/TE = 60/0.27 ms and resolution = 2 mm^3. SNR of sodium image in kidney volume was 31.7 ± 2.5 (N = 5).

[Results and conclusions] Using the high-sensitive DT coil, high-contrast sodium MR images were consistently obtained in kidneys in all 5 rabbits, which were well co-registered onto the proton anatomy images (**Fig. 1**). SNR was measured as ~32 in the kidney. The sodium concentration was the highest in central region of kidney; ranging from ~20 to ~145 mM (**Fig. 2B**). Group averaged sodium concentration in kidney volume was 78.1 ± 8.6 mM (N = 5) (**Fig. 2C**). High-resolution proton TSE images clearly depicted rabbit kidney anatomy – pelvis, medullar, cortex, and pelvic septa (**Figs. 3A** and **B**). The pelvic and pelvic septa regions were of low intensity in sodium MR imaging, while the medullar structures in inner and outer regions corresponded to the highest intensity structures (**Fig. 3C**). The measured sodium concentrations in cortex, inner-, and outer-medullar regions were 51.2 ± 10.0, 75.9 ± 15.7, and 107.3 ± 15.3 mM (N = 5), respectively. Profile of sodium concentration change from cortex to inner medullar is shown in **Figure 3E** – the measured gradient form cortex to inner medullar was ~6 mM/mm (N = 3). In conclusion, consistent measurements of sodium concentrations in normal rabbit kidneys were obtained using an in-house DT coil and UTE spiral sequence at 3T human scanner. A non-invasive assessment of alteration of corticomedullary sodium gradient may serve as an early indicator of renal pathology (e.g. acute tubular necrosis). Further comparison studies of sodium concentration between normal and renal malfunctioning kidney will be required to evaluate the clinical relevance of these measurements.

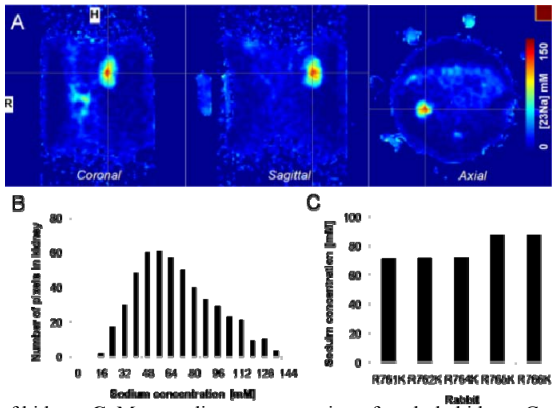

Fig. 2 Sodium MR imaging of rabbit kidneys. **A**, Coronal, sagittal, and axial views after correction of B_1 inhomogeneity field. **B**, Histogram of images of kidney. **C**, Mean sodium concentration of a whole kidney. Group averaged sodium concentration was 78.1 ± 8.6 mM (N = 5). Sodium concentration was the highest in the medullar region (e.g., > 100 mM) and reduced gradually toward the cortex.

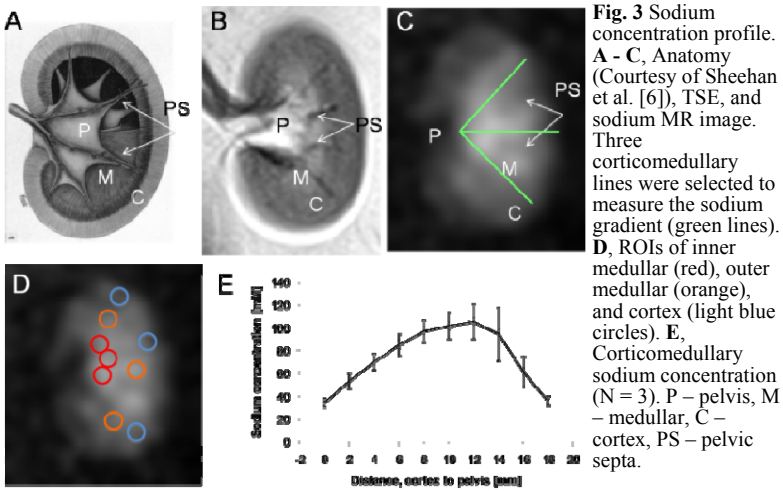

Fig. 3 Sodium concentration profile. **A - C**, Anatomy (Courtesy of Sheehan et al. [6]), TSE, and sodium MR image. Three corticomedullary lines were selected to measure the sodium gradient (green lines). **D**, ROIs of inner medullar (red), outer medullar (orange), and cortex (light blue circles). **E**, Corticomedullary sodium concentration (N = 3). P – pelvis, M – medullar, C – cortex, PS – pelvic septa.

[Reference] **1**. Atthe et al., *AJRP*, 297:1288-98 (2009). **2**, Wolf et al., *AJP*, 258:1125-31 (1989). **3**, Maril et al., *MRM*, 56:1229-34 (2006). **4**. Kim et al., *ISMRM*, 2011 submitted. **5**, Zhao et al., *ISMRM*, 2009. **6**, Sheenhan et al.,*Arch. Path.* 68:185-225 (1959). **[Acknowledgements]** Supported by RSNA Research Scholar grants RSCH1025.